Partial-Wave Analysis of the Inelastic Scattering of Electrons by Nuclei. I. Results for Quadrupole Excitations*

T. A. Griffy, D. S. Onley, J. T. Reynolds, and L. C. Biedenharn
Duke University, Durham, North Carolina

(Received June 1, 1962)

The problem of nuclear Coulomb excitation by inelastic scattering is approached by using a distorted partial-wave description for the initial and final states of the electron and a multipole expansion of the interaction with the nucleus which is treated in the semiclassical approximation. The method is facilitated by use of a closed analytic form for the contribution to the scattering of partial waves of sufficiently high angular momenta to be insensitive to the shape (but not the charge) of the target nucleus. The contribution of partial waves which do penetrate the nuclear charge distribution is found by numerical evaluation of the various matrix elements using electron wave functions obtained by numerical solution of the radial part of the Dirac equation in a central field. The particular case of electric quadrupole excitation assuming a uniform charge distribution is calculated and compared with the usual Born approximation treatment of inelastic electron scattering. The results of the calculations for 200-MeV electrons differ from the Born approximation result in two ways: for scattering angles less than 90° the Coulomb field causes an apparent, and significant, change in the radius of the charge distribution; for scattering angles greater than 90° the cross section differs *qualitatively* from the Born approximation result.

I. INTRODUCTION

THE use of high-energy electrons as a probe for the investigation of the excited states of nuclei has been the subject of much experimental[1–3] and theoretical[4,5] interest. High-energy electrons may be used to excite levels in the target nucleus of higher energies and angular momenta than may be reached in Coulomb excitation by nuclear projectiles. If the nuclear projectiles have sufficient energy to excite the higher states, penetration of the Coulomb barrier becomes important and nuclear reactions dominate Coulomb excitation. However, when electrons are used as projectiles, since the interaction is purely electromagnetic, this complication does not exist.

Previous theoretical treatments of inelastic electron scattering have been based on the Born approximation, i.e., the motion of the electrons is described by Dirac plane waves. This leads to the usual description of inelastic scattering in terms of a form factor for the nuclear transition. Explicitly, the Born approximation result for the differential cross section is

$$\sigma(\theta)=\sigma_m(\theta)\,|F(\mathbf{q})|^2, \tag{1.1}$$

where $\sigma_m(\theta)$ is the Mott scattering cross section. The nuclear form factor is given in terms of the transition charge density $\rho(\mathbf{r})$ by

$$F(\mathbf{q})=\int e^{i\mathbf{q}\cdot\mathbf{r}}\rho(\mathbf{r})d^3r. \tag{1.2}$$

The quantity $\mathbf{q}$ in Eq. (1.2) is the momentum transfer involved in the collision. Note that the momentum transfer includes that due to the scattering of the electron in the Coulomb field of the nucleus.

In the present treatment the effects of the static Coulomb field are included in the wave functions describing the motion of the electron. This is accomplished by employing a partial-wave expansion of the electron wave functions with the use of appropriate radial Coulomb wave functions. This type of analysis has the advantage that the momentum transfer due to the monopole interaction (the elastic scattering) is included in the wave functions.

Since the present treatment involves considerable numerical calculation, we do not propose that this type of analysis replace the usual Born approximation treatment. Rather, we hope that these results may be used to indicate the region of validity of the Born approximation, and offer an alternative approach to be used where the Born approximation fails. In particular, this type of calculation may be necessary for heavy nuclei where the effects of the Coulomb field of the nucleus should be particularly important.

II. DERIVATION OF CROSS SECTION

In this section, we derive an explicit formula for the differential cross section for the inelastic scattering of relativistic electrons. We employ a partial wave expansion for the electron wave functions and a multipole expansion for the electromagnetic interaction. In the present work, only the case of electric multipole excitations will be treated.

The Hamiltonian for electrons moving in a central potential $V(r)$ is given by[6]

$$H_0=\left[i\gamma_5\sigma_r\left(\frac{\partial}{\partial r}+\frac{1}{r}-\frac{\beta}{r}K\right)+V(r)+m\beta\right], \tag{2.1}$$

* Supported in part by the Army Research Office (Durham) and the National Science Foundation.

[1] W. C. Barber, F. Berthold, G. Fricke, and F. E. Gudden, Phys. Rev. **120**, 2081 (1960).
[2] H. Crannell, R. Helm, H. Kendall, J. Oeser, and M. Yearian, Phys. Rev. **123**, 923 (1961).
[3] R. H. Helm, Phys. Rev. **104**, 1466 (1956).
[4] L. I. Schiff, Phys. Rev. **96**, 765 (1954).
[5] H. B. Robl, Nuclear Phys. **2**, 641 (1956).
[6] M. E. Rose, *Relativistic Electron Theory* (John Wiley & Sons, Inc., New York, 1961).

where

$$K=\beta(\boldsymbol{\sigma}\cdot\mathbf{L}+1), \tag{2.2}$$

and

$$\sigma_r=\boldsymbol{\sigma}\cdot\hat{r}. \tag{2.3}$$

The total Hamiltonian may be written as a sum of H_0 and a term which describes the interaction of the electrons with the *nonstatic* part of the nuclear charge distribution. Following Schiff we employ the semiclassical treatment of the interaction, where the nuclear charge densities are treated as classical quantities. The interaction Hamiltonian matrix element then has the form

$$H_{\text{int}}=\int_{\text{nuclear volume}}\rho(\mathbf{r})\varphi(\mathbf{r})d\tau. \tag{2.4}$$

We have omitted from Eq. (2.4) the contribution of the interaction due to the nuclear currents $\mathbf{j}\cdot\mathbf{A}$. This term is of order v/c compared with the charge contribution, where v is some average nucleon velocity. The term will be particularly small for collective excitations where the velocity of an individual nucleon is small compared with c. The potential $\varphi(\mathbf{r})$ is that due to the passing electron; it may be written in terms of the Green's function as

$$\varphi(\mathbf{r})=\int\rho_e(\mathbf{r}')\frac{e^{i\omega|\mathbf{r}-\mathbf{r}'|}}{|\mathbf{r}-\mathbf{r}'|}d^3r', \tag{2.5}$$

where $\rho_e(\mathbf{r}')$ is given by $\Psi_f^\dagger\Psi_i$, Ψ_f, and Ψ_i being eigenstates of H_0. (Here ω is the energy of excitation.)

The eigenfunctions Ψ_i (Ψ_f) describe an incoming (outgoing) plane wave with an outgoing (incoming) scattered spherical wave due to the interaction $V(r)$. These wave functions may be expanded in terms of partial waves (angular momentum eigenstates) in the form (see Appendix)

$$\Psi^m=4\pi\left(\frac{E+m}{2EV}\right)^{\frac{1}{2}}\sum_{\kappa\mu}\exp(i\bar{\delta}_\kappa)i^l C_{\mu-mm\mu}{}^{l\frac{1}{2}j}\times Y_l{}^{\mu-m*}(\hat{p})\Psi_\kappa{}^\mu, \tag{2.6}$$

where V is the volume of normalization.

The Green's function in Eq. (2.5) may also be expanded in the usual form

$$\frac{e^{i\omega|\mathbf{r}-\mathbf{r}'|}}{|\mathbf{r}-\mathbf{r}'|}=4\pi i\omega\sum_{LM}j_L(\omega r_<)h_L{}^{(1)}(\omega r_>)\times Y_L{}^{M*}(\hat{r}_<)Y_L{}^M(\hat{r}_>). \tag{2.7}$$

The quantities $r_<$ and $r_>$ are the lesser and greater of r and r'.

Combining Eqs. (2.4), (2.5), and (2.7), we write H_{int} in the form

$$H_{\text{int}}=4\pi i\omega\sum_{LM}\int\int\rho(\mathbf{r})\Psi_f{}^\dagger(\mathbf{r}')\Psi_i(\mathbf{r}')j_L(\omega r_<)\times h_L{}^{(1)}(\omega r_>)Y_L{}^{M*}(\Omega_<)Y_L{}^M(\Omega_>)d^3r'd^3r. \tag{2.8}$$

If we assume that the nuclear transition charge density has the form

$$\rho(\mathbf{r})=\rho(r)Y_\lambda{}^\mu(\Omega), \tag{2.9}$$

and use the partial-wave expansion for the electron wave functions given in Eq. (2.6), the angular parts of the integral in Eq. (2.8) may be performed. This gives

$$H_{\text{int}}=8\left[\frac{(E_i+m)(E_f+m)}{E_iE_f}\right]^{\frac{1}{2}}\frac{1}{V}\sum_{\kappa\kappa'}\exp[i(\bar{\delta}_\kappa+\delta_{\kappa'})]\times i^{l-l'}(-)^{j'+\lambda+l+\frac{1}{2}}(2l+1)[(2\lambda+1)(2j+1)]^{\frac{1}{2}}\times C_{0mm}{}^{l\frac{1}{2}j}C_{m+\mu-m',m',m+\mu}{}^{l'\frac{1}{2}j'}C_{000}{}^{l\lambda l'}C_{m\mu m+\mu}{}^{j\lambda j'}\times W(j'l'jl;\tfrac{1}{2}\lambda)R(\kappa\lambda\kappa')Y_{l'}{}^{m+\mu-m'}(\hat{p}_f). \tag{2.10}$$

In deriving Eq. (2.10), we have made use of the equation

$$\int\chi_{\kappa'}{}^{\mu'*}Y_\lambda{}^\mu\chi_\kappa{}^m d\Omega=(-)^{j'+\frac{1}{2}+\lambda}\left[\frac{(2l+1)(2l'+1)(2j+1)}{4\pi}\right]^{\frac{1}{2}}\times C_{000}{}^{ll'\lambda}C_{m\mu\mu'}{}^{j\lambda j'}W(j'l'jl;\tfrac{1}{2}\lambda). \tag{2.11}$$

The quantity $R(\kappa\lambda\kappa')$ in Eq. (2.10) is the radial part of the integral in Eq. (2.8). Since the energy loss of the electron is small compared with its incident energy, the relation $(\omega/p)^2\ll1$ applies, and we may employ the long wavelength limit for the spherical Bessel and Hankel functions appearing in Eq. (2.8). The result for the radial integrals is then:

$$R(\kappa\lambda\kappa')=\int_0^\infty\int_0^\infty\rho(r)\times[f_\kappa(r')f_{\kappa'}(r')+g_\kappa(r')g_{\kappa'}(r')]\times r_<{}^\lambda r_>{}^{-\lambda-1}r^2r'^2drdr'. \tag{2.12}$$

The differential cross section is given in terms of H_{int} by the usual method of multiplication by the density of final states, division by the incident flux, and an average and sum over the initial and final spin projections. Performing these operations, we have

$$\sigma(\theta)=\frac{E_iE_f}{(2\pi)^2}\frac{p_f}{p_i}V^2\sum_{\mu mm'}|H_{\text{int}}|^2. \tag{2.13}$$

From Eqs. (2.13) and (2.10), we see that the calculation of the cross section has been reduced to the evaluation of the radial matrix elements $R(\kappa\lambda\kappa')$ given in Eq. (2.12). Having determined the radial matrix elements, the sum in Eq. (2.13) gives the cross section. The evaluation of the radial integrals is discussed in the next section.

III. RADIAL MATRIX ELEMENTS

The radial matrix elements defined by Eq. (2.12) are double integrals over the radial multipole operator $r_<^{\lambda}r_>^{-\lambda-1}$ times the radial parts of the nuclear transition charge density and the transition electron charge density. Under the simplifying assumption that the nuclear charge distributions are known for both the ground and excited states, and assuming that the effect of the nonspherical part of the excited state charge distribution on the electron wave functions may be neglected, the evaluation of these integrals becomes a matter of numerical integration. The Dirac-Coulomb functions appropriate to the given charge distributions are obtained from a numerical integration of the radial part of the Dirac equation. These functions are then multiplied by the transition charge distribution and the radial multipole operator and a numerical integration is performed to obtain the radial matrix elements.

While the procedure outlined above is conceptually quite simple, it is not feasible because of the large number of radial integrals required for the calculation of the cross section. It is essential to simplify the problem in some way without sacrificing the accuracy of the calculation.

The key to the simplification lies in the fact that one may divide the radial integrals into three groups according to the angular momenta of the electrons involved (i.e., according to the values of κ and κ'). The first group are those integrals corresponding to low values of $|\kappa|$ which depend sensitively on the size and shape of the nuclear charge distribution.

The second group are those integrals corresponding to electrons having intermediate values of $|\kappa|$ which, because of the angular momentum barrier, do not penetrate the nuclear charge distribution and hence the integrals are insensitive to its size and shape. The integrals in this second group are, consequently, well approximated by assuming that the nucleus is simply a point charge. The line of demarcation between group 1 and group 2 depends, of course, on the exact size and shape of the nuclear charge distribution as well as the energy of the scattering electron. For a typical case, $|\kappa|\sim 10$ gives a reasonable estimate for the boundary between the two groups.

The third group of integrals are those corresponding to large values of κ and hence to distant collisions. Because of the adiabatic nature of these distant collisions their contribution to the cross section is small and hence the integrals in group 3 may be neglected.

Another important simplifying approximation which can be made stems from the fact that the energy loss of the electron is small compared with the incident energy. For a typical case, say, 200-MeV electrons exciting a state of 1-MeV excitation, the energy loss is only 0.5%. This implies that to a good approximation, one may neglect the energy loss of the electron and assume that both the incident and outgoing electrons have the same energy. This approximation also has the important consequence that the radial integrals are now symmetric in the indices κ and κ' so that only half as many integrals need be computed.

The approximation of no energy loss yields important simplifications for the integrals in group 2. For the no energy loss, point nucleus limit the radial integrals may be expressed in closed form.[7] It seems more appropriate that the proof of this remark be given elsewhere in a systematic treatment of Coulomb integrals.[8] The method whereby these integrals are obtained is an extension of the contour integration techniques given for the corresponding nonrelativistic problem by Biedenharn, McHale, and Thaler.[9]

For electric quadrupole transitions the relevant integrals have the form:

$$\mathcal{I}_{\kappa\kappa'}=\int_0^\infty \frac{1}{r}g_\kappa(r)g_{\kappa'}(r)dr+\int_0^\infty \frac{1}{r}f_\kappa(r)f_{\kappa'}(r)dr, \quad (3.1)$$

where the radial wave functions are given explicitly by

$$\begin{Bmatrix} f_\kappa(r) \\ g_\kappa(r) \end{Bmatrix}=\begin{Bmatrix} -[(E-m)/(E+m)]^{\frac{1}{2}} \\ 1 \end{Bmatrix}(kr)^{\gamma-1}$$
$$\times\frac{2^\gamma e^{\pi y/2}|\Gamma(\gamma+iy)|}{\Gamma(2\gamma+1)}\begin{Bmatrix} \mathrm{Im} \\ \mathrm{Re} \end{Bmatrix}[(\gamma+iy)e^{i\varphi}e^{-ikr}$$
$$\times {}_1F_1(\gamma+1+iy,\,2\gamma+1,\,2ikr)], \quad (3.2)$$

with

$$\gamma=[\kappa^2-(\alpha Z)^2]^{\frac{1}{2}},$$
$$y=\alpha ZE/p, \quad (3.3)$$
$$e^{2i\varphi}=e^{-\pi i}(\gamma+iy)^{-1}(\kappa-i\alpha Zm/p),$$

and α is the fine structure constant. The integrals in Eq. (3.1) have distinct forms for $\kappa=\kappa'$ and $\kappa\neq\kappa'$, namely,

$$\int_0^\infty \frac{1}{r}[g_\kappa(r)]^2dr=4\frac{\Gamma(2\gamma-2)}{\Gamma(2\gamma+3)}\Big\{[\pi y+iy\psi(\gamma-iy)-iy\psi(\gamma+iy)]$$
$$\times\{(2\gamma^2-3\kappa+1)+(3y^2+\gamma^2-1)[1-(1-\beta^2)^{\frac{1}{2}}]\}+\gamma(2\gamma-1)(2\gamma+1)$$
$$-3\kappa(2\gamma-1)+3y^2(2\gamma-1)[1-(1-\beta^2)^{\frac{1}{2}}]+\frac{(\gamma-1)(2\gamma-1)}{\gamma^2+y^2}[\kappa\gamma-y^2(1-\beta^2)^{\frac{1}{2}}]\Big\}, \quad (3.4)$$

[7] M. E. Young and L. C. Biedenharn, Bull. Am. Phys. Soc. **5**, 112 (1960).
[8] J. T. Reynolds, D. S. Onley, and L. C. Biedenharn, J. Math. Phys. (to be published).
[9] L. C. Biedenharn, J. McHale, and R. M. Thaler, Phys. Rev. **100**, 376 (1955).

$$\int_0^\infty \frac{1}{r}[f_\kappa(r)]^2 dr = \left(\frac{1-(1-\beta^2)^{\frac{1}{2}}}{1+(1-\beta^2)^{\frac{1}{2}}}\right)\left\{\frac{8\Gamma(2\gamma-2)}{\Gamma(2\gamma+3)}\{3(\gamma^2+y^2)[\pi y+iy\psi(\gamma-iy)-iy\psi(\gamma+iy)]\right.$$
$$\left.+3y^2(2\gamma-1)+\gamma(2\gamma-1)(2\gamma+1)\}-\int_0^\infty \frac{1}{r}[g_\kappa(r)]^2 dr\right\}. \quad (3.5)$$

For $\kappa_1 \neq \kappa_2$:

$$\int_0^\infty \frac{1}{r}\begin{Bmatrix} f_{\kappa_1} f_{\kappa_2} \\ g_{\kappa_1} g_{\kappa_2} \end{Bmatrix} dr = \frac{48\pi\Gamma(\gamma_1+\gamma_2-2)}{\Gamma(\gamma_1+\gamma_2+3)\Gamma(3+\gamma_1-\gamma_2)\Gamma(3+\gamma_2-\gamma_1)\sin\pi(\gamma_2-\gamma_1)} \begin{Bmatrix} (E-m)/(E+m) \\ 1 \end{Bmatrix} \mathrm{Re}\{\cdots\}, \quad (3.6)$$

with

$$\{\cdots\} = \frac{\Gamma(\gamma_1+2+iy)\Gamma(\gamma_2-iy)}{|\Gamma(\gamma_1+iy)\Gamma(\gamma_2+iy)|}\exp i[\varphi_1+\varphi_2-\tfrac{1}{2}\pi(\gamma_2-\gamma_1)]\Bigg[(\gamma_1+2+iy)\sum_m \frac{(\gamma_2-\gamma_1-2)_m(-\gamma_1-\gamma_2-2)_m}{m!(-4)_m(-\gamma_1-2-iy)_m}$$
$$\times(\{\mp\}(-2)_m - e^{-2i\varphi_1}(-3)_m) + \{\mp\}e^{-2i\varphi_2}(\gamma_2-iy)\sum_m \frac{(\gamma_2-\gamma_1-2)_m(-\gamma_1-\gamma_2-2)_m}{m!(-4)_m(-\gamma_1-1-iy)_m}$$
$$\times(\{\mp\}(-1)_m - e^{-2i\varphi_1}(-2)_m)\Bigg]. \quad (3.7)$$

In the above equations, we have used the functions

$$\psi(z) = \frac{d}{dz}\ln\Gamma(z), \quad (3.8)$$

and

$$(a)_m = \Gamma(a+m)/\Gamma(a), \quad \beta = pc/E. \quad (3.9)$$

Although the analytic forms for the radial integrals given in Eqs. (3.4)–(3.7) have a very complicated appearance, the use of these results provides a very much faster method of computation than the numerical integration which must be used for the integrals in group 1.

We now consider the evaluation of radial integrals in group 1. Equation (2.12) may be reduced by integration over either r' (the electron coordinate) or r (the nuclear coordinate) leading to two equivalent forms:

$$R(\kappa\lambda\kappa') = R_0(\kappa\lambda\kappa') + \int_0^\infty \rho(r) P_{\kappa\kappa'}(r) dr, \quad (3.10)$$

or

$$R(\kappa\lambda\kappa') = \int_0^\infty \psi_{\kappa\kappa'}(r') C(r') dr', \quad (3.11)$$

where

$$R_0(\kappa\lambda\kappa') = \int_0^\infty \rho(r) r^{\lambda+2} dr \int_0^\infty \psi_{\kappa\kappa'}(r') r'^{-\lambda+1} dr', \quad (3.12)$$

$$P_{\kappa\kappa'}(r) = r^{-\lambda+1}\int_0^r \psi_{\kappa\kappa'}(r') r'^{\lambda+2} dr' - r^{\lambda+2} \times \int_0^r \psi_{\kappa\kappa'}(r') r'^{-\lambda+1} dr', \quad (3.13)$$

$$C(r') = r'^{\lambda+2}\int_{r'}^\infty \rho(r) r^{-\lambda+1} dr + r'^{-\lambda+1}\int_0^{r'} \rho(r) r^{\lambda+2} dr, \quad (3.14)$$

$$\psi_{\kappa\kappa'}(r) = f_\kappa(r) f_{\kappa'}(r) + g_\kappa(r) g_{\kappa'}(r). \quad (3.15)$$

The term R_0 is essentially the contribution of a point nucleus to the scattering. Here, the transition charge distribution $\rho(r)$ provides a constant factor, which is essentially the λ-pole moment of the charge distribution, independent of κ and κ'. The integral over the radial wave functions is of the same form as that for the point case. As these wave functions are distorted by the finite charge distribution, we cannot claim that this integral is independent of the shape of $\rho(r)$ but it is readily seen to approximate $\mathcal{I}_{\kappa\kappa'}$ especially for large values of κ. The second term of Eq. (3.10) is the major contributor of finite size effects to the radial integral. The function $P_{\kappa\kappa'}(r)$ as it appears in Eq. (3.10) is a penetration function designating the region of $\rho(r)$ which contributes to the radial integral. In the alternative expression [Eq. (3.11)] the integral over the radial wave functions is cut off near the origin by the function $C(r')$ [defined explicitly in Eq. (3.14)] which depends only on the shape of $\rho(r)$. This serves to define a region around the origin in the space of the electron coordinate which is excluded from the integral. The shapes of these functions will be discussed more fully in Sec. V for particular cases.

IV. NUMERICAL PROCEDURES

In this section we outline those parts of the calculation where the numerical procedures are of interest or where the accuracy of these has to be considered. The problem falls naturally into two parts: (1) The evaluation of the radial integrals and; (2) The calculation of the cross section.

The numerical calculation of radial integrals in group 1 (see Sec. III) is accomplished by reducing the problem to sets of simultaneous linear differential equations which are then solved by the method of Runge-Kutta-Gill.[10] This method, although rather lengthy, is in-

[10] F. Edelman, IBM Tech. Newsletter **13**, 52 (1957).

trinsically stable which is a necessary requirement in view of the great variety of functions we encounter.

We require two Coulomb potential functions arising from the charge distributions $\rho_1(r)$ and $\rho_2(r)$ for the initial and final states, respectively.[11] These functions $V_1(r)$ and $V_2(r)$ are calculated from the set of linear equations:

$$\begin{aligned}&\frac{d}{dr}X_i(r)=-r\rho_i(r),\\&\frac{d}{dr}Y_i(r)=r^2\rho_i(r),\\&V_i(r)=-\alpha Z[r^{-1}Y_i(r)+X_i(r)-X_i(R)]/Y_i(R),\\&\qquad i=1,2,\end{aligned}\tag{4.1}$$

which are integrated from $r=0$ to $r=R$, being for this purpose any point outside the charge distribution in which region $V_i(r)=-\alpha Z/r$.

The Dirac radial wave functions f_κ and g_κ satisfy the coupled differential equations given in the Appendix [Eq. (A4)]. For any given radial integral we have to solve two such pairs, one each for the initial and final states which differ, in general, in the value of κ, of the energy E, and of the potential function $V(r)$. The boundary conditions for these functions is established at the origin at which point we start the integration. The behavior of $f_\kappa(r)$ and $g_\kappa(r)$ near the origin is readily seen to be

$$\begin{aligned}&f_\kappa(r)\sim r^{\kappa-1},\\&g_\kappa(r)\sim r^{\kappa},\qquad \text{for}\quad \kappa>1,\end{aligned}\tag{4.2}$$

provided $V(r)$ is not singular. It is advantageous for numerical calculation to define:

$$\begin{aligned}&f_\kappa(r)=r^{\kappa-1}F_\kappa(E,m,r),\\&g_\kappa(r)=r^{\kappa}G_\kappa(E,m,r),\qquad \text{for}\quad \kappa>1,\end{aligned}\tag{4.3}$$

and solve instead the equations for F_κ and G_κ:

$$\begin{aligned}&\frac{d}{dr}F_\kappa(E,m,r)=[V(r)-E+m]rG_\kappa(E,m,r),\\&\frac{d}{dr}G_\kappa(E,m,r)=\frac{1}{r}\{-(2\kappa+1)G_\kappa(E,m,r)\\&\qquad-[V(r)-E-m]F_\kappa(E,m,r)\},\end{aligned}\tag{4.4}$$

which may be derived from (4.3). The boundary conditions are

$$\begin{aligned}&F_\kappa(E,m,0)=F_0\ \text{(arbitrary)},\\&G_\kappa(E,m,0)=\frac{E+m-V(0)}{2\kappa+1}F_0,\\&\left(\frac{d}{dr}F_\kappa\right)_0=\left(\frac{d}{dr}G_\kappa\right)_0=0.\end{aligned}\tag{4.5}$$

For $\kappa\leqslant 1$ we find

$$\begin{aligned}&f_\kappa(r)=-r^{|\kappa|}G_{|\kappa|}(E,-m,r),\\&g_\kappa(r)=r^{|\kappa|-1}F_{|\kappa|}(E,-m,r).\end{aligned}\tag{4.6}$$

Normalization of the wave functions and determination of the phase shifts is achieved by comparison of the calculated values of f_κ and g_κ with their asymptotic forms at some large value $r=R$:

$$\begin{aligned}\begin{Bmatrix}f_\kappa(r)\\g_\kappa(r)\end{Bmatrix}&\sim\frac{1}{pr}\left(1+\frac{\xi}{8p^2r^2}\right)\\&\times\begin{Bmatrix}-\left(\frac{E-m}{E+m}\right)^{\frac{1}{2}}\sin\left(pr+\delta_\kappa+\frac{\xi}{2pr}-\frac{\xi y}{4p^2r^2}\right)\\\cos\left(pr+\delta_\kappa+\frac{\xi}{2pr}-\frac{\xi y}{4p^2r^2}\right)\end{Bmatrix},\end{aligned}\tag{4.7}$$

where

$$\begin{aligned}&\xi=\kappa^2+(\alpha mZ)^2/p^2,\\&y=\alpha ZE/p,\\&p^2=E^2-m^2.\end{aligned}$$

We have neglected terms $O[(pR)^{-3}]$ in Eq. (4.7).

The radial integral $R(\kappa\lambda\kappa')$ may be calculated from Eq. (3.10) which in the linear differential form may be written

$$\begin{aligned}&\frac{d}{dr}X(r)=\psi_{\kappa\kappa'}(r)r^{\lambda+2},\\&\frac{d}{dr}Y(r)=\psi_{\kappa\kappa'}(r)r^{-\lambda+1},\\&\frac{d}{dr}Z(r)=[r^{-\lambda+1}X(r)-r^{\lambda+2}Y(r)]\rho(r),\\&R(\kappa\lambda\kappa')=QY(R)+Z(a),\end{aligned}\tag{4.8}$$

where $Q=\int_0^\infty\rho(r)r^{\lambda+2}dr$ and a is the nuclear radius. The alternative form for the radial integral [Eq. (3.11)] may be similarly reduced.

The number of calculations to be performed may be decreased by making various simplifying assumptions. If the electron mass may be neglected in comparison

[11] Under the simplifying assumption that the nuclear wave functions have the same radial dependence in both the initial and final states, both $\rho_1(r)$ and $\rho_2(r)$ may be identified with $\rho(r)$ defined in Eq. (2.9).

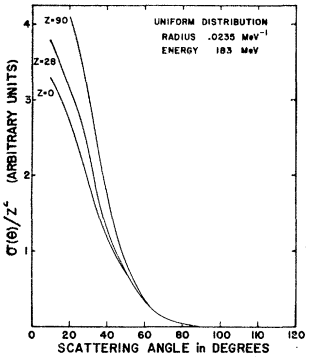

FIG. 1. Differential cross section for inelastic electron scattering compared for different nuclear charges. The factor Z^2 has been removed.

with its energy, we see from Eqs. (4.3), (4.6), and (3.15) that

$$\psi_{\kappa\kappa'}(r)=\psi_{-\kappa-\kappa'}(r). \tag{4.9}$$

Where it is possible to assume the same radial dependence for the initial and final-state charge distributions $[\rho_1(r)=\rho_2(r)]$ and neglect energy loss ($E_1=E_2$) in the collision, the product of the wave functions has the additional symmetry:

$$\psi_{\kappa\kappa'}(r)=\psi_{\kappa'\kappa}(r). \tag{4.10}$$

The same symmetry relations clearly hold for the radial integrals $R(\kappa\lambda\kappa')$.

Once the radial integrals are known, the evaluation of the cross section is easily performed by means of Eqs. (2.10) and (2.13). The Clebsch-Gordan coefficients are evaluated using the algebraic forms given by Condon and Shortley[12] and the Racah coefficients are calculated from the algebraic forms given by Biedenharn, Blatt, and Rose.[13]

In order to speed the convergence of the series in Eq. (2.10), we made use of the reduced series as defined by Yennie *et al.*[14] Their method is based on the recursion relation for the Legendre polynomials. If

$$f(\theta)=\sum a_l P_l(\cos\theta),$$

then from the recursion relation for $P_l(\cos\theta)$ we have

$$(1-\cos\theta)f(\theta)=\sum a_l' P_l(\cos\theta),$$

where

$$a_l'=a_l-\frac{l+1}{2l+3}a_{l+1}-\frac{l}{2l-1}a_{l-1}.$$

For large l, $a_l'=O(|a_l|/l^2)$ so that the reduced series converges considerably faster than the original series.

In order to test our numerical procedures, calculations of limiting cases were performed. The first test was the evaluation of the cross section for the quadrupole excitation of a point nucleus with $Z=0$. As is well known, the differential cross section for this case is simply proportional to $\cos^2(\theta/2)$.[5] We find that the numerical results obtained from the program differ from $\cos^2(\theta/2)$ by less than 1 part in 10^5.

A more critical test of the program is the ability to reproduce the Born form factor for a finite size nucleus.

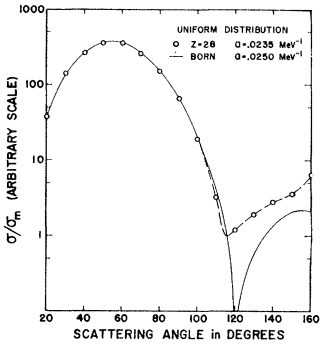

FIG. 3. The form factor for inelastic electron scattering with $Z=28$ compared with a Born form factor.

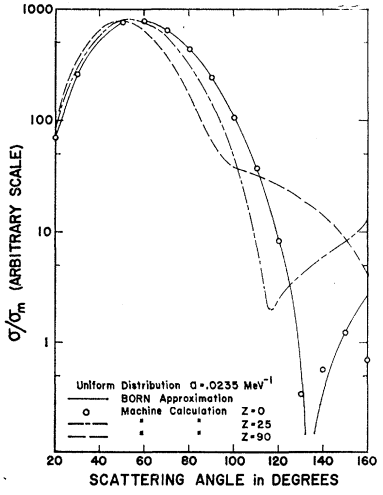

FIG. 2. The form factor for inelastic electron scattering on a logarithmic scale. The solid curve is the analytic Born form factor compared with the machine calculation denoted by circled points. (Note that the label $Z=25$ in the figure should read $Z=28$.)

In our analysis the Born approximation corresponds to putting $Z=0$. However, because of the finite size of the nucleus, we must still employ the numerical procedures given above to evaluate the radial integrals and hence we obtain a test of the methods used to calculate these integrals.

A comparison of the results of a numerical calculation of the form factor for a uniform distribution with the corresponding Born approximation form factor is shown in Fig. 2. The solid line is the (analytic) Born result and the circles represent the numerical results obtained using the methods given above. The comparison is quite good except at the very backward angles where the partial wave expansion is sensitive to the exact cancellation of different terms in the series.

V. DISCUSSION OF RESULTS

We have performed calculations of the inelastic scattering cross section for the case of electric quadru-

[12] E. U. Condon and G. H. Shortley, *Theory of Atomic Spectra* (Cambridge University Press, New York, 1935).

[13] L. C. Biedenharn, J. M. Blatt, and M. E. Rose, Revs. Modern Phys. **24**, 249 (1952).

[14] D. R. Yennie, D. G. Ravenhall, and R. N. Wilson, Phys. Rev. **95**, 500 (1954).

pole excitations, using the numerical methods described in Sec. IV. Some typical results are shown in Figs. 1 and 2 where we show the cross section and form factor obtained from the calculations using a uniform charge distribution of radius $a=4.7$ F and an incident energy of 183 MeV. In addition, we have neglected the mass of the electron compared with its kinetic energy. The radius was the same for all three curves labeled $Z=0$, 28, and 90 shown in the figures. It is, of course, unreasonable to assume the same size charge distributions for $Z=28$ and 90. However, since our primary purpose was an investigation of the effects due to finite charge (deviations from the Born approximation) we felt that the most reasonable comparison was that of the same size nucleus having different values of Z. The curves are normalized to have the same value at the maximum to facilitate a comparison of their shapes. We have taken into account the contribution of the first 27 partial waves including the modification due to the finite size of the charge distribution in the first 9 of these.

One sees from Fig. 2 that the main effect of the finite charge is to displace the peak in the form factor toward

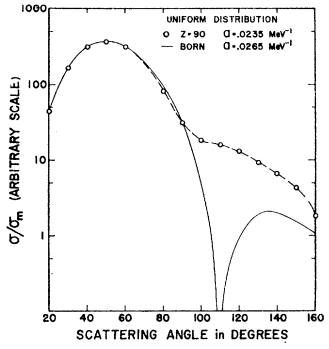

FIG. 4. The form factor for inelastic electron scattering with $Z=90$ compared with a Born form factor.

smaller angles and to fill in the diffraction minimum in the Born form factor (the $Z=0$ curve). Since an increase in the radius a also has the effect of shifting the peak in the form factor toward smaller angles, we see from Fig. 2 that for angles $<90°$ increasing Z has the same effect as increasing the radius of the charge distribution. The effect of increased radius *vs* increased Z is further illustrated by Figs. 3 and 4 where we show the form factors obtained from the numerical calculation with $Z=28$ and 90 and also the Born form factors with radii of $a=5.0$ F and $a=5.3$ F, respectively. The two curves are seen to coincide quite well for angles $<90°$ indicating that *in the forward direction the primary effect of the Coulomb distortions is to increase the apparent size of the charge distribution.*[15] This effect is of the order of 10 to 15% for $Z=90$ and is approximately proportional to $Z^{\frac{1}{3}}$.

[15] A similar effect has been noted in the phase-shift calculations of electron scattering. See, for example, reference 14 and R. Hofstadter, Revs. Modern Phys. **28**, 214 (1956).

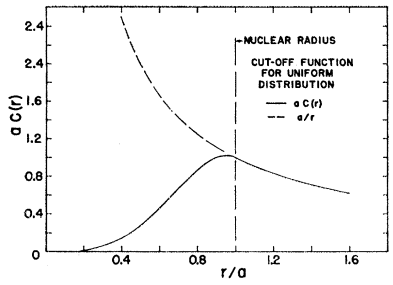

FIG. 5. The cutoff function $C(r)$ [defined by Eq. (3.14)] for a uniform charge distribution with radius a, as a function of r/a. The dashed curve corresponds to a point nucleus.

We now investigate some of the qualitative effects of the finite size of the charge distribution on the radial integrals. As was indicated in Sec. III, the double radial integrals may be written in two equivalent forms, depending on the order of integration chosen. One form for the radial integral is

$$R(\kappa\lambda\kappa')=\int_0^\infty \psi_{\kappa\kappa'}(r')C(r')dr'. \tag{3.11}$$

In Fig. 5, we show the behavior of $C(r')$ for the case of a uniform charge distribution. From Fig. 5 we see then, as was pointed out in Sec. III, that the effect of the finite size of the nucleus is to "cut off" the contribution to the integrals of the region inside the charge distribution.

Doing the radial integration in the opposite order, we obtain

$$R(\kappa\lambda\kappa')=R_0(\kappa\lambda\kappa')+\int_0^\infty \rho(r)P_{\kappa\kappa'}(r)dr. \tag{3.10}$$

This form of the radial integral is useful in obtaining information about the "probing" of the charge distribution by the various partial waves. The function $P_{\kappa\kappa'}(r)$ is approximately independent of the form of the charge distribution. The amount of overlap in the integral between this function and $\rho(r)$ then tells us how sensitive the radial integral is to the shape of the charge distribution. In Fig. 6, we show some typical results for $P_{\kappa\kappa'}(r)$. Figure 6 indicates that it is only the low values of κ and κ' that are sensitive to the size and shape of the

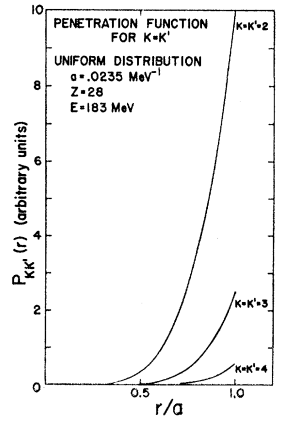

FIG. 6. The penetration function $P_{\kappa\kappa'}(r)$ [defined by Eq. (3.13)] for a uniform charge distribution with radius a, as a function of r/a.

charge distribution. For large values of κ and κ' the "probing function" is essentially zero for small values of r and hence the value of the radial integral is insensitive to the shape of the charge distribution. It is this property of the "probing function" which allows us to use the radial integrals for a point charge for the higher values of κ.

In summary we may conclude that the Coulomb field of the nucleus affects the cross section for inelastic electron scattering in the following ways: For angles less than 90°, the Coulomb field causes an apparent change in the radius of the charge distribution, the effect being about 15% for $Z=90$; for angles greater than 90° the cross section differs qualitatively from the Born approximation cross section.

Further calculations of this type are in progress. We are investigating the dependence of the cross section on the shape of the transition charge distribution and we are also attempting to find some approximate techniques which will simplify the calculation and at the same time allow us to retain the essential features.

ACKNOWLEDGMENTS

The computations reported here were performed at the Duke University Computing Center, which is supported in part by the National Science Foundation, on an IBM 7070 digital computer. We are indebted to Dr. Gallie and his staff for their cooperation.

We also wish to acknowledge the assistance of Neal Huffaker in some of the preliminary calculations.

APPENDIX

In this section, we discuss the partial wave expansion of the eigenstates of the unperturbed Hamiltonian

$$H_0=\left[i\gamma_5\sigma_r\left(\frac{\partial}{\partial r}+\frac{1}{r}-\frac{\beta}{r}K\right)+V(r)+m\beta\right]. \quad \text{(A1)}$$

The form of the solutions is, of course, well known (see, e.g., reference 6). The discussion presented here is primarily to establish the notation and conventions used in the text.

The eigenstates of equation (A1) with total energy E may be written in the form

$$\psi_\kappa{}^\mu=\begin{Bmatrix} g_\kappa(r)\chi_\kappa{}^\mu \\ if_\kappa(r)\chi_{-\kappa}{}^\mu \end{Bmatrix}. \quad \text{(A2)}$$

The spin angle functions $\chi_\kappa{}^\mu$ are given explicitly by

$$\chi_\kappa{}^\mu=\sum_\tau C_{\mu-\tau\tau\mu}{}^{l\frac{1}{2}j}Y_l{}^{\mu-\tau}(\hat{r})\chi^\tau. \quad \text{(A3)}$$

The functions $\chi_\kappa{}^\mu$ are eigenfunctions of the total angular momentum j and the orbital angular momentum l, with eigenvalues $j=|\kappa|-\frac{1}{2}$ and $l=\kappa$ for $\kappa>0$, $l=-\kappa-1$ for $\kappa<0$.

The radial wave functions $f_\kappa(r)$ and $g_\kappa(r)$ are solutions to the coupled differential equations

$$\frac{df_\kappa}{dr}=\frac{\kappa-1}{r}f_\kappa-[E-m-V(r)]g_\kappa(r), \quad \text{(A4a)}$$

$$\frac{dg_\kappa}{dr}=(E+m-V)f_\kappa(r)-\frac{\kappa+1}{r}g_\kappa(r), \quad \text{(A4b)}$$

which have the asymptotic behavior

$$f_\kappa(r)\sim-\left(\frac{E-m}{E+m}\right)^{\frac{1}{2}}\frac{1}{pr}\sin(pr+\delta_\kappa), \quad \text{(A5a)}$$

$$g_\kappa(r)\sim\frac{1}{pr}\cos(pr+\delta_\kappa). \quad \text{(A5b)}$$

We now form the appropriate combination of the solutions $\psi_\kappa{}^\mu$ to describe an incident plane wave plus outgoing Coulomb scattered waves. We assume that the electrons are polarized with eigenvalue of the polarization operator $O_z=\pm\frac{1}{2}$.[6] The partial wave expansion is then

$$\psi^m=4\pi\left(\frac{E+m}{2E}\right)^{\frac{1}{2}}\sum_{\kappa\mu}\exp(i\delta_\kappa)_i{}^lC_{\mu-mm\mu}{}^{l\frac{1}{2}j}\times Y_l{}^{\mu-m^*}(\hat{p})\psi_\kappa{}^\mu. \quad \text{(A6)}$$

The phase $\bar{\delta}_\kappa$ is given by:

$$\bar{\delta}_\kappa=\delta_\kappa-y\ln 2pr+(l+1)\pi/2, \quad \text{(A7)}$$

where $y=\alpha ZE/p$. Equation (A6) is the partial wave expansion used in the text [Eq. (2.6)].